^{129}Xe NMR Studies of Hyper-Cross-Linked Polyarylcarbinols: Rigid Versus Flexible Structures

C. Urban,[1] E. F. McCord,* O. W. Webster, and L. Abrams

DuPont Co., Central Research and Development, Experimental Station, Wilmington, Delaware 19880-0269[2]

H. W. Long, H. Gaede, P. Tang,[3] and A. Pines

Department of Chemistry, University of California, Berkeley, California 94720

Received January 3, 1995. Revised Manuscript Received April 17, 1995[⊗]

Xenon NMR is used with adsorption measurements to infer information about the microstructure of some novel hyper-cross-linked polyarylcarbinols. It is shown that rigid-rod connecting units are necessary for microporosity in these systems, as hyper-cross-linked polymers based on flexible structures are found to have conventional surface areas and xenon NMR spectra. A microporous polymer based on rigid triarylcarbinol monomers shows high xenon uptake and a linear chemical shift variation with pressure at room temperature. Spin–lattice relaxation and cross-polarization dynamics are studied at low temperatures. In this regime the xenon has extremely long equilibration times, and the adsorption dynamics are complicated but give important insight into the polymer topology. The data are compared with two possible models of the polymer microstructure.

Introduction

The search for new polymer topologies and architectures is driven by the need to improve the thermal and mechanical properties of known polymers, as well as the desire to develop completely new polymer chemistry. Often the physical and chemical properties of these new structures prove to be superior to those of existing materials.

Hyper-cross-linked polyarylcarbinols,[4–6] comprised of a framework of rigid-rod connecting units held together by trifunctional tie points, represent such a new topology and give rise to a number of unusual properties, such as microporosity and swellability. Scheme 1 shows the synthesis of hyper-cross-linked polymer **1**. Due to the nature of the cross-linking process, a structural framework possessing a large internal void volume is formed. This results in surface areas as high as 1000 m^2/g, which compares with other high surface area materials like carbon black. In addition, these hyper-cross-linked polymers, unlike other highly cross-linked materials, swell 200–300% in most organic solvents. This unique combination of high surface area and controlled cavities of molecular dimensions yields promising new materials for use as catalyst supports and adsorbents.

The unusual swelling behavior of these new cross-linked polymers is poorly understood, and since they neither dissolve nor melt, very little information is available concerning their detailed pore structure and morphology. One explanation, model 1 (Figure 1), involves the formation of highly cross-linked particles having a high microporosity during the early polymerization stages which give rise to the observed high surface area. These micro-gel particles (with diameter estimated to be 100–300 Å) cross-link later in the polymerization reaction via more or less loose cross-links, rendering the resulting material insoluble. These loose cross-links would, according to this model, allow for some flexibility between the cross-linked particles and account for the observed high swellability.[6]

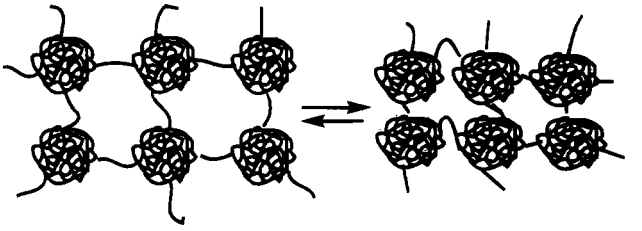

Figure 1. Schematic explanation of the swelling behavior of a polymer with a morphology of soluble micro-gel particles that are cross-linked via flexible linkages.

Alternatively, in model 2 (Figure 2), the swelling can be explained based on the assumption that the solvent-filled micropores which are formed during polymerization contract when the polymer is dried and the solvent evaporates. Since the network structure is rigid, the pores cannot collapse completely, thus imposing a very high stress on the dry network. To release this stress, the cross-linked polymers swell, even in thermodynamically poor solvents, in order to regain the conformation they had during the cross-linking reaction, i.e., it is thermodynamically favorable to fill the pores with solvent and thus release stress. Such a model was

⊗ Abstract published in *Advance ACS Abstracts,* June 1, 1995.

(1) Present address: Hempel A/S, Lundtoftevej 150, DK2800 Lyngby, Denmark.

(2) Contribution number 7050.

(3) Department of Chemical Engineering.

(4) Webster, O. W.; Gentry, F. P.; Farlee, R. D.; Smart, B. E. *Polym. Prepr. (Am. Chem. Soc., Div. Polym. Chem.)* **1991**, *32*, 412.

(5) Webster, O. W.; Kim, Y. H.; Gentry, F. P.; Farlee, R. D.; Smart, B. E. *Polym. Prepr. (Am. Chem. Soc., Div. Polym. Chem.)* **1992**, *33*, 186.

(6) Webster, O. W.; Gentry, F. P.; Farlee, R. D.; Smart, B. E. *Makromol. Chem., Macromol. Symp.* **1992**, *54/55*, 477.

0897-4756/95/2807-1325$09.00/0

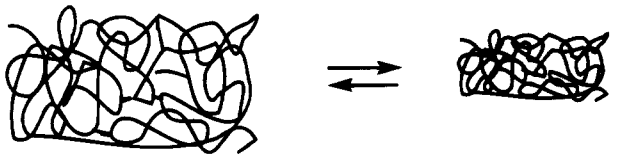

Figure 2. Schematic explanation of the swelling behavior of a polymer with a homogeneous morphology.

proposed by Davenkov et al.,[7] to explain the swelling of polystyrene-based hyper-cross-linked materials. The main difference between these two models is that the first assumes loosely cross-linked microporous particles, implying two different pore sizes or distributions (micropores within the particles and larger pores between them), whereas the latter implies a homogeneous polymer with a uniform pore size distribution throughout the polymer.

^{129}Xe NMR spectroscopy is a very useful method for investigating the microstructure of porous materials such as zeolites,[8,9] and confined spaces in clathrates,[10] as well as for characterizing polymers.[11-15] A wide range of xenon NMR studies has recently been reviewed, including applications of both thermally and optically polarized xenon.[16] The ^{129}Xe chemical shift depends on the frequency and type of collisions that the xenon atoms undergo. In zeolites the chemical shift strongly depends on both temperature and pressure and is characteristic of size, shape, and chemical composition of the zeolite pore. In some cases the xenon–xenon interactions are known to be the dominant parameter determining the chemical shift anisotropy[17] or the isotropic chemical shift.[18] Xenon NMR has been used to characterize polymer blends,[15,19,20] amorphous polymer regions,[12] nascent polymerized material on catalyst surfaces,[14] cross-linked elastomers,[13] and, with optical polarization, polymer surfaces.[21] Reported values of the chemical shifts of xenon dissolved in polymers range from 185 to 245 ppm at pressures from 2 to 12 atm.[22] There is very little pressure dependence to the chemical shift of xenon in polymers.[22] Most workers use very high pressures (8–12 atm) to obtain sufficient xenon dissolved in the polymer to give an observable xenon NMR signal. In phase-separated polymer blends two signals can be seen if the domain size in the blend is larger than about 0.6 μm (and the chemical shift of xenon is different in the two components of the blend).[15]

Scheme 1

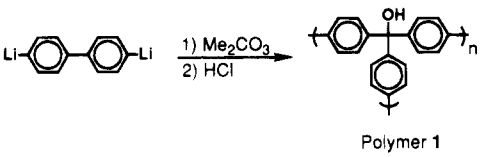

Scheme 2

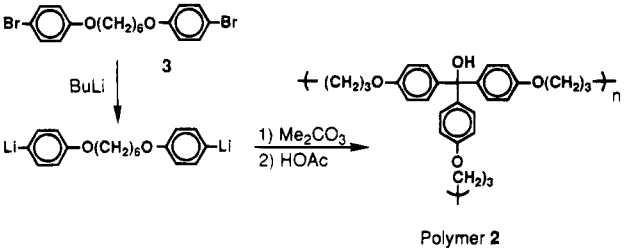

In the present study, ^{129}Xe NMR spectroscopy was used to investigate hyper-cross-linked polymers, focusing on two different polymer types: polymer **1** (Scheme 1), which has rigid biphenyl moieties as connecting units between the tiepoints, and polymer **2** (Scheme 2), with flexible connections. The latter polymer was synthesized to investigate whether a rigid connection unit is needed for obtaining a high surface area, i.e., to stabilize the voids between the tie points. Additional studies on polymer **1** were performed to determine the microstructure of the system in the context of the two models discussed above.

Experimental Section

Synthesis. Hyper-cross-linked polymer **1** was prepared as described previously.[6] Hyper-cross-linked polymer **2**, which has not been described previously, was synthesized using the following procedure.

Step 1: 1,6-Bis(4-bromophenoxy)hexane, **3**. Dry sodium carbonate (52.5 g) and a few crystals of potassium iodide were added to a solution of 46.5 g (0.269 mol) 4-bromophenol in 150 mL of acetone. The mixture was heated to reflux, and a solution of 46.4 g of 1,6-dibromohexane in 50 mL of acetone was added dropwise. The reaction mixture was then refluxed for 12 h. An extra 150 mL of acetone was added and refluxing was continued. After 46 h an extra 19.6 g (0.113 mol) of 4-bromophenol was added in 20 mL of acetone together with 5.0 g of potassium carbonate. After 12 h 100 mL of ethyl acetate were added, and the resulting mixture was refluxed for 20 min. After cooling to room temperature and stripping, the solids were washed with saturated potassium carbonate solution, water, and 3 N NaOH. The organic phase was dried, concentrated, and combined with solids formed during the NaOH extraction. Recrystallization from 2-propanol yielded 13.9 g (24.1%) of an off-white **3**. ^{1}H NMR (360 MHz, $CDCl_3$) δ/ppm 1.55 (m, 2.5 H), 1.81 (m, 2 H), 3.96 (t, 2 H), 6.78 (d, 2 H), 7.37 (d, 2 H). EI MS *m/z* 428 ($M^{\bullet+}$), 255 ({M − OC6H4Br}$^+$).

Step 2: A solution of 11.7 mmol 1,6-Bis(4-bromophenoxy)-hexane in 150 mL of anhydrous THF was cooled under nitrogen to −70 °C using a dry ice/acetone bath. To the clear, colorless solution 47 mmol of *tert*-butyllithium (1.7 M in hexane) were added, adjusting the addition rate to maintain the temperature of the reaction mixture below −68 °C. After stirring the mixture at −70 °C for 30 min, a solution of 7.18 mmol of dimethyl carbonate in 20 mL of THF was added, adjusting the addition speed to keep the reaction temperature

(7) Davenkov, V. A.; Tsyurupa, M. P. *Polym. Mater. Sci. Eng.* **1992**, *66*, 146.
(8) Ito, T.; Fraissard, J. *Zeolites* **1988**, *8*, 350.
(9) Dybowski, C.; Bansal, N.; Duncan, T. M. *Annu. Rev. Phys. Chem.* **1991**, *42*, 433.
(10) Ripmeester, J. A. *J. Am. Chem. Soc.* **1982**, *104*, 289.
(11) Sefcik, M. D.; Schaefer, J.; Desa, J. A. E.; Yelon, W. B. *Polym. Prepr. (Am. Chem. Soc., Div. Polym. Chem.)* **1983**, *24*, 85.
(12) Stengle, T. R.; Williamson, K. L. *Macromolecules* **1987**, *20*, 1428.
(13) Kennedy, G. J. *Polym. Bull.* **1990**, *23*, 605.
(14) Ferrero, M. A.; Webb, S. W.; Conner, W. C.; Bonardet, J. L.; Fraissard, J. *Langmuir* **1992**, *8*, 2269.
(15) Walton, J. H.; Miller, J. B.; Roland, C. M. *J. Polym. Sci., Part B: Polym. Phys.* **1992**, *30*, 527.
(16) Raftery, D.; Chmelka, B. F. In *NMR, Basic Principles and Progress*; Springer-Verlag: Berlin, 1994; Vol. 30, p 11.
(17) Springuel, M. A.; Fraissard, J. *Chem. Phys. Lett.* **1989**, *154*, 299.
(18) Chmelka, B.; Raftery, D.; Levine, R.; Pines, A. *Phys. Rev. Lett.* **1991**, *66*, 580.
(19) Brownstein, S. K.; Roovers, J. E. L.; Worsfold, D. J. *Magn. Reson. Chem.* **1988**, *26*, 392.
(20) Walton, J. H.; Miller, J. B.; Roland, C. M.; Nagode, J. B. *Macromolecules* **1993**, *26*, 4052.
(21) Raftery, D.; Reven, L.; Long, H.; Pines, A.; Tang, P.; Reimer, J. A. *J. Phys. Chem.* **1993**, *97*, 1649.
(22) Miller, J. B.; Walton, J. H.; Roland, C. M. *Macromolecules* **1993**, *26*, 5602.

below −68 °C. After the addition was completed, the reaction mixture was stirred at −70 °C for another hour and allowed to warm to room temperature over night. The reaction was then quenched with 30 mL of methanol, neutralized with acetic acid to pH 6, and filtered. The solid polymer was washed thoroughly with water, acetone, and THF and dried in vacuum for 24 h. Yield: 1.5 g (31%). Elemental analysis yielded the following results: Calcd for $(C_{28}H_{31}O)_n$: C, 77.93%; H, 7.24%; O, 14.83%. Found: C, 78.39%; H, 7.31%; O, 14.76%.

NMR Sample Preparation. Two sealed samples of polymer **1** and one sealed sample of polymer **2** were prepared. For the first sealed sample of polymer **1** (prepared at DuPont), ca. 500 mg of the polymer was weighed into an NMR tube (10 mm diameter, Wilmad Glass Co. 513-8 PPM with constriction, narrowed to fit the manifold) and were degassed while heating at ca. 200 °C in high vacuum (≪0.11 Torr) for several days. After cooling the sample to room temperature, it was pressurized with 600−900 Torr of Xe gas (Air Products, research grade 99.995%). The sample was allowed to equilibrate for 15 min and cooled in liquid nitrogen, and then the NMR tube was flamed off. Polymer **1** was pressurized to about 778 Torr. The sample of polymer **2** was prepared similarly, except that it was pressurized to about 724 Torr of xenon gas.

The second sealed sample of polymer **1** (prepared at Berkeley) was evacuated at $<10^{-5}$ Torr while heating at 40−60 °C for several hours before loading with xenon (80% enriched, Isotec Inc.) at a pressure of 375 Torr (confirmed by comparison with chemical shift vs pressure data in Figure 5).

NMR Measurements. ^{129}Xe NMR spectra of the first sealed sample of polymer **1** and of polymer **2** were obtained at DuPont on a Varian VXR 400 at 110.63 MHz (unlocked) using a spectral width of 50 kHz, an acquisition time of 0.64 s, a recycle delay of 5 s, and a 52° pulse at either 20 or −100 °C ± 0.5 °C. Proton decoupling was not used. Typically 1000 transients were collected, and a line broadening of 20 Hz was used. In polymer **1**, the signal obtained using a 52° pulse and a 1 s delay was about 50% of that using a 60 s delay; using a 5 s delay the signal was 80% of that using a 60 s delay. A 5 s delay was chosen for the spectra reported here. No additional signal was detected in the spectrum of this sample of polymer **1** under these conditions of preparation and measurement. The spectra of polymer **1** were externally referenced using the head-space gas in a sample of NaY zeolite pressurized to about 542 Torr with xenon gas; the chemical shift of this xenon gas was set to 0.36 ppm. This procedure should reference the spectra to xenon gas (zero pressure, 25 °C) at 0 ppm.[23] The xenon NMR spectrum of polymer **2** was referenced by setting the sharp xenon gas resonance near 0 ppm to 0.48 ppm (value determined by the head-space pressure above the sample).

Measurements on the second sealed sample of polymer **1** were made at Berkeley either on a Nalorac spectrometer operating at 51.4 MHz or a Chemagnetics based spectrometer operating at 49.5 MHz. Typical acquisition parameters were a sweep width of 40 kHz, recycle delay of 15 s (at ambient temperature) or 60 s (at low temperatures), using 6 μs 90° pulses. All spectra were referenced to low-pressure xenon gas. The low-temperature experiments were preceded by an experiment in an empty cell of optically pumped xenon at very low pressure (ca. 20 Torr). This provides directly a temperature-independent reference since the correction from this state is negligible. The variable-pressure measurements, as well as the experiments performed by introducing the xenon directly at low temperatures, were made on additional samples of polymer **1** and used the optically pumped xenon NMR spectrometer that has been previously described elsewhere.[21,24] Such a setup allows in situ variable-pressure measurements to be performed rapidly and accurately over a range of temperatures. Temperature measurements were accurate to ±2 °C with a precision of ±0.5 °C, and chemical shift measurements have a precision of 1 ppm (slightly less at low temperatures due to broader lines and lower signal to noise).

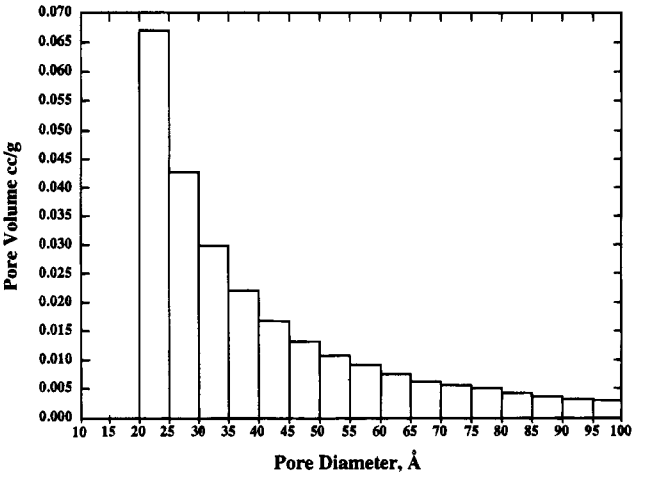

Figure 3. Pore size distribution data for polymer **1**.

Surface Area Measurements. Surface area measurements were made using the adsorption of nitrogen at its boiling point via the BET method.[25] A Micrometrics ASAP 2400 adsorption apparatus was used to measure the amount of nitrogen sorbed. The pore size distribution, shown in Figure 3, was calculated using the nitrogen desorption isotherm (assuming cylindrical pores) according to the BJH method.[26]

Results

The surface area of the polymer **1** was measured by the BET method to be 914 ± 25 m^2/g (834 ± 25 m^2/g on a second batch of the polymer), as reported earlier.[6] The pore size distribution data calculated from the N_2 desorption isotherms are shown in Figure 3. These data show that 40% of the pores in this material have a nominal pore diameter <20 Å. The newly synthesized hyper-cross-linked polymer **2** shows no indication of microporosity; the BET surface area of 2 m^2/g (error −0.2 to +0.1 m^2/g) can be attributed to the macroscopic surface of the polymer particles. No significant swellability in common organic solvents (such as tetrahydrofuran, chloroform, or methanol) was observed.

The uptake of Xe gas by the polymer samples was calculated from the drop in Xe pressure when the evacuated sample tube was connected to a storage bulb. The uptake of Xe gas by the polymers studied was as follows:

polymer	gas uptake (mL/g polymer)
1	41
2	2 (ref 27)

^{129}Xe NMR spectra were recorded for polymer **1** (first sealed sample, ~778 Torr) at 20 and −100 °C (Figure 4) and for polymer **2** at 20 °C (Figure 5). The chemical shift of the xenon resonance found for polymer **1** changes from 152 ppm at room temperature to about 168 ppm at −100 °C. The line width at half-height increases from 804 Hz at 20 °C to 964 Hz at −100 °C. A signal in the region of 200 ppm was not seen for this sample even

(23) Jameson, C. J.; Jameson, A. K.; Cohen, S. *J. Chem. Phys.* **1973**, *59*, 4540.
(24) Raftery, D.; Long, H.; Grandinetti, P. J.; Meersmann, T.; Reven, L.; Pines, A. *Phys. Rev. Lett.* **1991**, *66*, 584.
(25) Brunauer, S.; Emmett, P. H.; Teller, E. *J. Am. Chem. Soc.* **1938**, *60*, 309.
(26) Barret, E. P.; Joyner, L. G.; Halenda, P. P. *J. Am. Chem. Soc.* **1951**, *73*, 373.
(27) Zero uptake of xenon gas within the experimental error of 2−3% absolute.

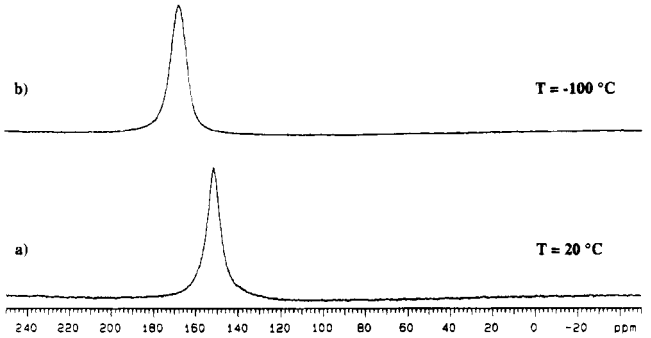

Figure 4. ^{129}Xe NMR spectra of rigid hyper-cross-linked polytriarylcarbinol (polymer **1**, sample 1) at (a) 20 and (b) −100 °C.

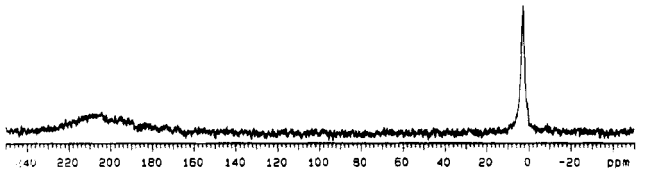

Figure 5. ^{129}Xe NMR spectra of flexible hyper-cross-linked polymer **2** at 20 °C.

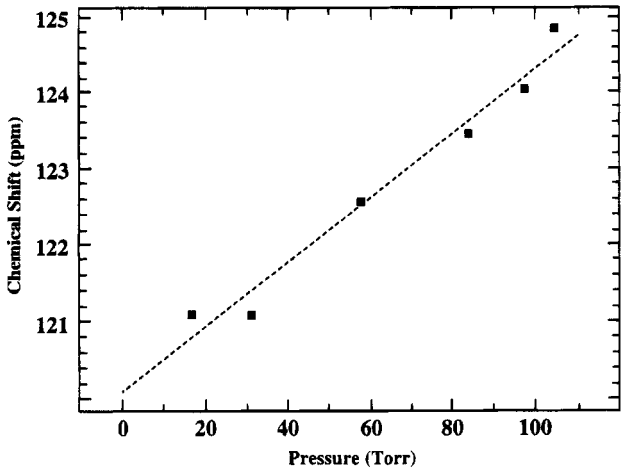

Figure 6. Chemical shift vs pressure of xenon in polytriarylcarbinol (polymer **1**) at room temperature.

after 6000 transients using a 10 s delay. Due to the low Xe uptake of polymer **2** (vide supra), in comparison to that of polymer **1**, a poorer signal-to-noise ratio was observed in the xenon NMR spectrum of polymer **2** (Figure 5). The broad peak at around 206 ppm is barely visible in the noise of the baseline. There is a small sharp peak attributable to xenon gas which was set to 0.48 ppm and a much larger, broader peak slightly downfield of this, at about 3.0 ppm. For this sample, the reference chemical shift scale obtained from the zeolite/gas standard was shifted 1.87 ppm so that the xenon gas peak was at 0.48 ppm rather than at −1.39 ppm.

The xenon chemical shift in polymer **1** as a function of pressure measured at room temperature is shown in Figure 6. The intercept is 120.1 ppm and the slope is 0.04 ppm/Torr (30 ppm/atm) and is linear in the range shown, but at higher pressures, above about 600 Torr it begins to show some negative curvature in contrast to the strictly linear behavior observed in zeolites with monovalent cations. Some negative curvature is seen

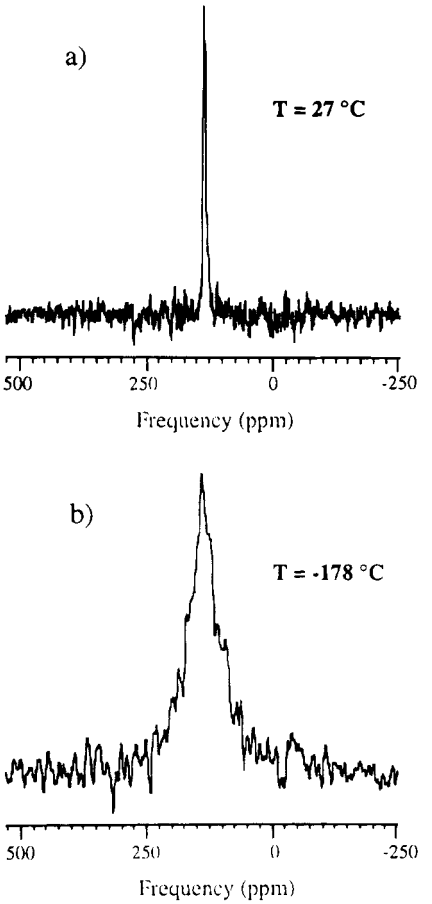

Figure 7. ^{129}Xe spectra of xenon in the sealed sample of polytriarylcarbinol (polymer **1**) at a pressure of 375 Torr at (a) 23 and (b) −178 °C.

in pure xenon studies at high densities (>100 amagats).[28]

In the second sealed sample of polymer **1** (375 Torr of xenon), the line width was measured to be 300 Hz which is comparable to the line width measured in the higher pressure sample after correcting for the difference in field strength. The chemical shift was measured to be 135 ppm at room temperature. At low temperature the chemical shift increases only slightly, reaching 149 ppm at −178 °C, the lowest temperature that can be obtained on our variable-temperature xenon probe. The line width increases sharply below −130 °C and is equal to approximately 4.5 kHz at −178 °C (Figure 7). Here the motion of the xenon is clearly being reduced, and the xenon is no longer rapidly averaging over many pores. There was no discernible change in the line width when using high-power proton decoupling; therefore, the line width is presumably dominated by a chemical shift distribution due to the different sites and pore sizes within the polymer.

The sealed samples in all of the above experiments were slowly cooled in the probe (typical cooling rates were ≈0.3 °C/s below −100 °C) and allowed to thermally equilibrate for 5−10 min at the set temperature. Experiments were also performed on this polymer using a setup designed for optically polarized xenon work where the experimental procedure is quite different. Full details of the methodology have been previously de-

(28) Jameson, C. J.; Jameson, A. K.; Gutowsky, H. *J. Chem. Phys.* **1970**, *53*, 2310.

scribed.[21] Briefly, the sample is connected to a vacuum system and a xenon reservoir while in the probe; the sample is allowed to equilibrate at the set temperature, and then an aliquot of xenon is added (occasionally several aliquots for variable pressure studies). For optically polarized xenon the spectra are acquired a few seconds later (within the T_1 of the xenon) after the pressure has stabilized. The question of equilibration in such experiments is a vexing one, although for some low surface area materials (<20 m^2/g, nonporous), it has been reasonably well established.[29] For a microporous material, however, a few seconds is clearly insufficient, especially at low temperatures. Migration times may be on the order of hours in systems such as carbon black. However, we show below that the xenon establishes a quasi-static equilibrium within a few minutes that shows no time dependence on a time scale of hours at some temperatures. This observation allows an investigation of the nonequilibrium dynamics in this system, albeit a qualitative one.

We note that experiments with optically polarized xenon allow one to follow the real-time adsorption on a much faster time scale when the NMR is monitored with small tipping angle pulses after adding the xenon. Some experiments of this kind were performed,[29] which showed transient freezing of the xenon in the bulk and much broader adsorbed peaks. However these experiments are extremely sensitive to the quantity of xenon added and cannot be adequately reproduced. Therefore only data acquired via signal averaging in "quasi-static" equilibrium will be considered in this paper.

Figure 8 shows the results of an experiment displaying the dramatic nonequilibrium effects in this system. Xenon is added at room temperature to a sample of polymer **1**, and the system is slowly cooled to −168 °C (typical cooling rates were ≈0.3 °C/s below −100 °C). The xenon spectrum at this point in time is shown in Figure 8a and is quite similar to the low-temperature spectrum of the sealed sample (Figure 7b). Next a second aliquot of xenon is added; 5 min later the spectrum in Figure 8b is obtained (average of four scans, 4 min acquisition time). The second peak corresponding to the xenon just added is at ~250 ppm, about 100 ppm higher than the equilibrated xenon! This spectrum showed no changes over a 2 h period, which in itself is a powerful demonstration of equilibration times in high surface area materials. The sample is then warmed to −152 °C and after another 5 min equilibration period the spectrum in Figure 8c is obtained. Both peaks have narrowed somewhat and the "nonequilibrium" peak has shifted to ~235 ppm. Again no time dependence is seen over a 1 h period. The sample should be singular is then heated again, this time to −124 °C; at this temperature the peaks have begun to coalesce and the spectra are definitely time dependent. Two representative spectra are shown: Figure 8d is taken 15 min after reaching the set temperature and Figure 8e is taken 45 min later.

This behavior was found to be irreversible, that is recooling the sample did not result in the return of a second peak. Recooling resulted in the "normal" behavior seen in the sealed samples of polymer **1**, that is, a slight downfield shift and increased line width. Furthermore, in a separate experiment, the procedure was

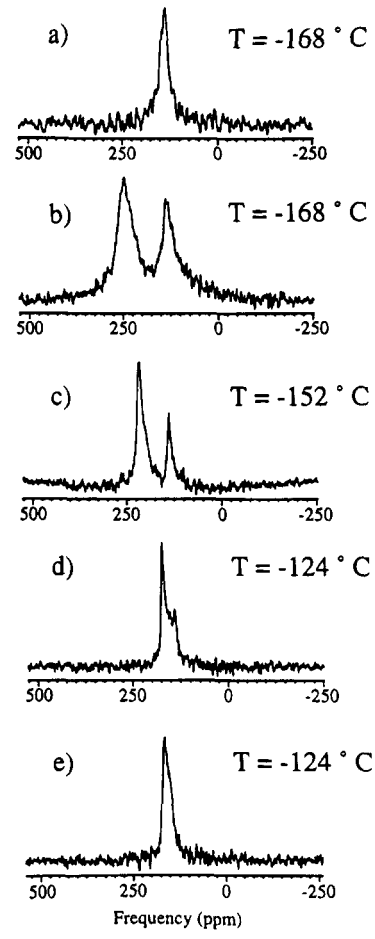

Figure 8. Low-temperature spectra of xenon adsorbed in polytriarylcarbinol (polymer **1**). An aliquot of xenon is loaded at room temperature and the sample is slowly cooled to −168 °C. (a) Spectrum just *before* loading the second aliquot; (b) spectrum 5 min *after* adding the second aliquot; (c) spectrum 5 min after warming to −152 °C; (d) spectrum 15 min after warming to −124 °C; (e) spectrum 45 min after warming to −124 °C.

repeated (with identical results) up to the state represented by Figure 8c and then cooled back to the original temperature (−168 °C). The nonequilibrium peak remained at the position it attained at −152 °C, and thus even the shifts of the well-separated peaks are irreversible. The intensity ratio of the two peaks remained constant.

At low temperatures, where the two xenon peaks are completely separated, an inversion recovery experiment was performed. The data show a large difference between the spin−lattice relaxation times of the two sites (Figure 9). A least-squares fit to a semilog plot of the data (Figure 10) shows that the low frequency ("equilibrium") peak has a T_1 of 12.5 s, about one-half that of the high-frequency ("nonequilibrium") peak, 24.0 s. As discussed below the cross-polarization data indicate that the heteronuclear dipolar coupling with the protons is approximately equal in the two sites, indicating that fluctuating chemical shift anisotropy is the most likely relaxation mechanism.

Despite the apparent lack of effect of proton decoupling in reducing the line width, dipolar contact exists between the xenon and proton spin systems at temperatures below about −140 °C, as proven by successful proton-to-xenon cross-polarization experiments. Figure 11 shows a typical magnetization buildup curve for the

(29) Long, H. W. Ph.D. Thesis, University of California at Berkeley, 1993.

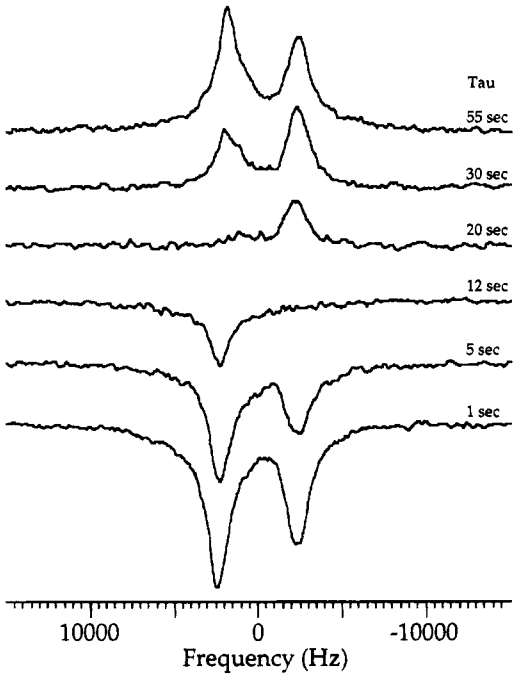

Figure 9. Representative inversion–recovery data of xenon in polytriarylcarbinol (polymer **1**) at $T = -168$ °C. Xenon was added at two different temperatures as in the procedure described for Figure 8.

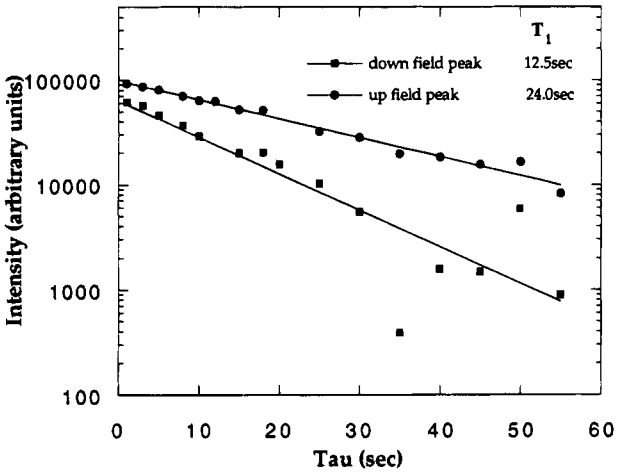

Figure 10. Semilog plot of all of the inversion recovery data. The ordinate is the integrated intensity of the xenon peaks; the solid lines represent least-squares fits to the data.

xenon with the growth due to polarization transfer, followed by the onset of exponential decay due to spin–lattice relaxation in the rotating frame. The figure only shows one site, but both peaks could be cross polarized and the contact time dependence was similar with an optimal contact time determined to be 5 ms at −168 °C.

Finally, polarization transfer from optically pumped xenon to protons has been performed in this sample.[30] This study has shown a slight contact time dependence of the proton line width indicating that protons with the strongest dipolar coupling to xenon also have the largest homonuclear dipolar coupling.

(30) Long, H. W.; Gaede, H. C.; Shore, J.; Reven, L.; Bowers, C. R.; Kritzenberger, J.; Pietrass, T.; Pines, A.; Tang, P.; Reimer, J. A. *J. Am. Chem. Soc.* **1993**, *115*, 8491.

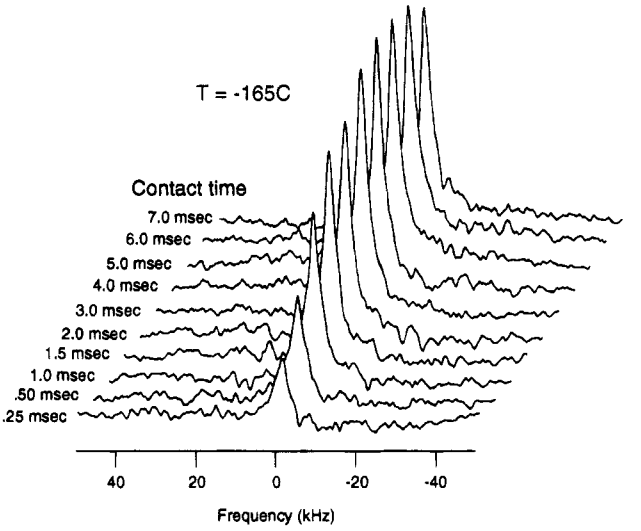

Figure 11. Stack plot of the spectra obtained for various cross polarization contact times in polytriarylcarbinol (polymer **1**).

Discussion

Polymer 2, Flexible Cross-Links. One of the guidelines for the construction of high surface area hyper-cross-linked polymers is the use of rigid connection units. To verify this concept, the flexible monomer **3** was synthesized and, after conversion to the bis-dilithio derivative, was cross-linked according to the procedure used for the synthesis of **1**[6] to give polymer **2**.

Unlike the rigid polymer, which polymerizes to give a 100% yield of insoluble material,[6] a yield of around 30% insolubles was obtained for polymer **2**. This is presumably due to the better solubility of the flexible monomer unit, rendering low molecular weight microgel particles soluble which were insoluble when constructed with a rigid biphenyl link. In addition, due to the flexibility of the monomer, it is very likely that a considerable amount of cyclic structures, closed loops, are formed by an intramolecular reaction of the reactive ends on the surface of the growing particle. This cyclization corresponds to a termination process not present when using rigid monomers (polymerization in both cases is carried out in a fairly dilute solution), terminating the polymerization at a rather low molecular weight; thus, not all of the growing polymer particles actually grow to a large-size insoluble network. Only the insoluble material was used for the experiments described here.

The ^{129}Xe NMR spectrum of polymer **2** (Figure 5) shows a broad resonance with low signal-to-noise at around 206 ppm and a large sharper signal at about 3 ppm. This 206 ppm chemical shift is typical of xenon gas dissolved in a polymer. The signal at around zero ppm is very similar to that observed for xenon interacting with the surface of poly(acrylic acid) at room temperature.[21] There are two components to this ~0 ppm signal, a distinct signal for free xenon gas which is not interacting with the sample, presumably in the void spaces between polymer particles, and a second larger, slightly downfield, signal. This larger signal is due to the xenon gas in contact with the sample which is rapidly exchanging between the gas phase and the surface adsorbed phase. From the much lower signal to noise of the xenon signal at 206 ppm as compared to

the xenon signal in the spectrum obtained using polymer **1**, the characteristic shape of the signal near 0 ppm, and the chemical shift of 206 ppm, it can be concluded that some xenon atoms are either dissolved to a small extent in the polymer or located in a few randomly formed pores and that the major interaction of xenon gas with this polymer is a weak surface adsorption with a low surface area material. Combined with the negligible uptake of xenon gas of this polymer, this confirms the result found by surface analytical techniques: no microporosity is present when a flexible monomer is employed.

The flexible hyper-cross-linked polymer **2** shows no significant swelling and is not microporous. This demonstrates that, for the formation of high-surface-area hyper-cross-linked polymers, rigid connection units between the cross-links are necessary, similar to hyper-cross-linked polystyrene networks.[7] These rigid cross-links are needed to build micropores of a molecular size that are held in shape and cannot collapse.

Polymer 1, Rigid Cross-Links. This polymer shows a chemical shift that is consistent with xenon gas in micropores, rather than dissolved in a bulk polymer. This is further supported by the high xenon uptake observed and the higher signal-to-noise ratio at about 1 atm xenon pressure of the xenon NMR signal (Figure 4). The pressure dependence of the chemical shift at room temperature makes it clear that the xenon occupies an interconnected pore volume where xenon–xenon collisions occur. The small change in chemical shift with decreasing temperature is characteristic of microporous substances and is due to the large number of surface collisions that occur even at room temperature. The increase in line width as the temperature is lowered has been observed for both polymers and zeolites.[31,32] It suggests site heterogeneity; sites with different chemical shifts are observed as the exchange rate of xenon between these sites is reduced at the lower temperature.

The chemical shift data for the high surface area polymer **1** at low temperatures are interpreted using the established empirical guidelines for xenon NMR.[8] The chemical shift can be represented as the following function of density (ϱ) when the adsorption sites are weak:

$$\sigma = \sigma_0(T,r) + \sigma_1(T)\varrho + L \qquad (1)$$

Here the chemical shift in the limit of low density, σ_0, is explicitly written as a function of temperature (T) and pore size (r). Although the explicit functional dependence on r is not known, σ_0 is empirically found from zeolite studies to be inversely dependent on pore size.[8] It is therefore tempting to assign the two peaks as resulting from two different pore sizes; however, it is very difficult to rationalize why the xenon should exclusively occupy large pores when in thermodynamic equilibrium with the polymer. Due to the greater van der Waals interaction (overlap) with the surface having greater curvature, the xenon should occupy the smaller cages if the intrinsic adsorption energies of the different cage sizes are the same. There also appears to be no structural rationalization for having small pores only on the surface of the polymer particles, where the xenon that is rapidly introduced at low temperatures first comes into contact with the polymer.

An alternative explanation of the data lies in the second term of eq 1. When the xenon initially comes into contact with the polymer at low temperatures, it cannot diffuse rapidly through the pore network into the particles; otherwise it would equilibrate. Thus the xenon must be kinetically trapped in pores at or near the surface. The local density of xenon in these pores may be quite high, and, if there are several xenon atoms per pore, then the xenon–xenon interactions can cause the large observed chemical shift. Cheung and co-workers[31] have observed nonequilibrium xenon resonances in zeolites, which they attributed to a macroscopic xenon density gradient introduced by rapid cooling. They have observed a chemical shift difference between the equilibrium site and the nonequilibrium site of about 25 ppm. This effect disappears at 144 K (−129 °C) in about 20 min. They have attributed the nonequilibrium chemical shift as arising from a xenon dimer in a nonequilibrium distribution. Our results are quite similar to theirs at our highest temperature (−124 °C). The major difference between our experiments and theirs is that Cheung and co-workers believe that a temperature gradient existed in their sample due to rapid cooling, while our samples are at a uniform temperature and still display nonequilibrium behavior. In our case, we see a nonequilibrium peak which differs from the equilibrium peak by about 30 ppm at −124 °C and are attributing the nonequilibrium resonance to xenon in large pores near the surface. At lower temperatures, we see a much larger (100 ppm) difference in chemical shift between the equilibrium and nonequilibrium peaks, with the nonequilibrium chemical shift at about 250 ppm. There are precedents for shifts of this magnitude from several studies. Xenon occluded in NaA zeolite shows a series of peaks in the NMR spectrum due to the discrete, resolved distribution of xenon pore occupancies.[18,33] This system has a well-defined cage diameter of 11.4 Å. One xenon/cage has a resonance at ~75 ppm reflective of the interaction with the cage. Two xenons/cage is at ~95 ppm, etc., up to seven xenons/cage at 225 ppm; thus, in this system, xenon–xenon interactions increase the observed chemical shift by 150 ppm. In studies of spin polarized xenon adsorbed onto poly(acrylic acid) at low temperatures, the chemical shift in the limit of zero coverage was 95 ppm but increased at high coverage to over 195 ppm.[21] Clearly xenon–xenon interactions can be of comparable magnitude to xenon–surface interactions. Unfortunately it is extremely difficult to quantify the xenon pore occupancy in these experiments even in the bulk, let alone purely at surface sites. Measurement times for xenon isotherms would clearly be prohibitively long at these temperatures due to the equilibration times involved (i.e., no observable progress toward equilibrium on a 2 h time scale). Qualitatively, however, this model provides a plausible mechanism to describe the adsorption behavior. After the xenon has been added at low temperatures and during the subsequent warming (Figure 8c–e) the xenon gradually begins to diffuse into

(31) Cheung, T. T. P.; Fu, C. M.; Wharry, S. *J. Phys. Chem.* **1988**, *92*, 5170.
(32) Cheung, T. T. P. *J. Phys. Chem.* **1990**, *94*, 376.
(33) Larsen, R.; Shore, J.; Schmidt-Rohr, K.; Emsley, L.; Long, H.; Pines, A.; Janicke, M.; Chmelka, B. *Chem. Phys. Lett.* **1992**, *214*, 220.

the particle. This leads to fewer xenon–xenon interactions and thus a decrease of the chemical shift until the interactions are on the same order as the "equilibrium" xenon distributed throughout the particle. This model explains directly why the behavior is irreversible as the equilibration process increases the entropy of the system.

It is possible to speculate on how the different relaxation times could be rationalized by this model. If the relaxation is dominated by fluctuating chemical shift anisotropy, the xenon atoms in the highly occupied cages have a much smaller effective volume to move in and thus a shorter correlation time. In the short correlation time limit the relaxation time is inversely proportional to the correlation time and thus xenon atoms in these cages (the pores with high xenon occupancy at higher chemical shift) will have a longer spin–lattice relaxation time, as observed experimentally. The greater homonuclear dipolar interaction in the filled cages will most likely not contribute to the relaxation, even with the enriched xenon used in some of the experiments, as the T_1 in pure frozen xenon is extremely long (tens of minutes at least) over the entire temperature (and thus correlation time) range of the solid.[34] Experiments at different magnetic field strengths would have to be done to substantiate this possible relaxation mechanism.

The two models for the microporous polymer discussed in the Introduction differ somewhat subtly in terms of their effect on xenon NMR spectra. The model assuming loosely cross-linked micro-gel particles (Figure 1) implies two different environments, one within the gel particle and the other in the voids between the gel particles. However, given the presumed size of the micro-gel particles (100–300 Å), fast exchange will undoubtedly lead to a single average line which is to be expected from the homogeneous model as well. At low temperatures the xenon will most likely equilibrate within the smallest pores of both models. However, the low-temperature adsorption of xenon and the observed nonequilibrium adsorption dynamics (Figure 8) can give a means to distinguish between the polymer topologies of the two models. When the xenon is rapidly introduced at low temperatures, it must be trapped at or near the exposed surface of the polymer. In the homogeneous model the external surface area would be only ~10 m^2/g for 10 μm diameter particles and would not be sufficient to rapidly sorb all of the xenon. In the micro-gel model the external surface area of the particles would likely be in excess of 100 m^2/g and the larger void spaces would allow the xenon to access more of this surface. Thus in the micro-gel model the bottle neck for xenon adsorption is not entering the pore system, but diffusion within it, as appears to be the case experimentally. However, other possibilities such as an unusual surface structure cannot be ruled out. Experiments on this system at higher pressure would be desirable, especially if the loading could be calibrated. It might also be interesting to study the xenon dynamics in a solvent swelled system, as one reviewer has suggested.

(34) Yen, W. M.; Norberg, R. E. *Phys. Rev.* **1963**, *131*, 269.

Conclusions

The comparison between polymer **1** with rigid cross-links and polymer **2** with flexible cross-links makes it clear that only the former is microporous, and thus rigid-rod cross-links are necessary for these hyper-cross-linked materials to have ultrahigh surface area. The adsorption of xenon at low temperatures in microporous samples is dramatically far from equilibrium and does not even approach equilibrium on the time scale of hours. The interpretation of the NMR data supports a polymer topology of a micro-gel of highly porous particles loosely cross-linked together forming larger voids between them.

Acknowledgment. The DuPont group would like to thank K. Zilm for suggesting the xenon NMR approach at DuPont, C. Dybowski and M. Smith for their help and advice, K. Raffell for technical assistance, and D. Corbin for a NaY zeolite sample. The help of P. J. Krusic and S. A. Hill with the preparation of the NMR samples and of J. Quill with preparation of this paper is highly appreciated. The Berkeley group thanks D. Raftery for help in the initial optical pumping experiments on this sample and Prof. J. Reimer for a fruitful collaboration and reading of an early draft of this paper. H.G. acknowledges NSF for a fellowship and P.T. acknowledges IBM for financial support. The Berkeley work was supported by the Director, Office of Energy Research, Office of Basic Energy Sciences, Material Sciences Division of the U.S. Department of Energy under Contract DE-AC03-76SF00098.

CM950003O